

Reversible C₆₀ Binding to Dendrimer-Containing Ir(CO)Cl(PPh₂R)₂ Complexes

Vincent J. Catalano* and Nicholas Parodi

Department of Chemistry, University of Nevada, Reno, Nevada 89557

Received October 18, 1996[®]

The phosphine compounds PPh₂(G-1) and PPh₂(G-2), where G-1 is 3,5-bis(benzyloxy)benzyl and G-2 is 3,5-bis((3,5-bis(benzyloxy)oxy)benzyl), were synthesized. The complexes, *trans*-Ir(CO)Cl(PPh₂(G-1))₂, **1**, and *trans*-Ir(CO)Cl(PPh₂(G-2))₂, **2**, show reversible binding with C₆₀. Thermodynamic data on the reversible binding were obtained in chlorobenzene by line width analysis of the ³¹P{¹H} NMR spectra. The activation parameters Δ*G*₂₆₅[‡] (kcal mol⁻¹), Δ*H*[‡] (kcal mol⁻¹), and Δ*S*[‡] (cal mol⁻¹ K⁻¹) were calculated as 1.3, 18, and 20 for **1**·C₆₀ and 1.3, 24, and 42 for **2**·C₆₀. The thermodynamic quantities Δ*G*₂₆₅[°] (kcal mol⁻¹), Δ*H*[°] (kcal mol⁻¹), and Δ*S*[°] (cal mol⁻¹ K⁻¹) were determined to be -2.8, -25, and -105 for **1**·C₆₀ and -3.0, -18, and -57 for **2**·C₆₀. The rates of reaction with O₂ for **1** and **2** were measured and are comparable to that for *trans*-Ir(CO)Cl(PPh₃)₂ under similar conditions. The compound PdI₂(PPh₂(G-1))₂, **3**, does not show reversible binding with C₆₀. Crystal structures were obtained for **1** (*a* = 10.218(1) Å, *b* = 12.731(3) Å, *c* = 13.116(2) Å, α = 112.05(1)°, β = 108.30(1)°, γ = 102.22(1)°, *V* = 1392.2(4) Å³) and **3** (*a* = 10.243(2) Å, *b* = 12.689(2) Å, *c* = 13.146(2) Å, α = 112.33(1)°, β = 108.96(1)°, γ = 101.23(1)°, *V* = 1392.4(4) Å³).

Introduction

The coordination of fullerenes, particularly C₆₀, to late transition metal complexes is well-known.¹ Coordination of Vaska's compound, *trans*-Ir(CO)Cl(PPh₃)₂, and its analogs is by far the most widely studied.² In all these cases the metal is bound to the fullerene in an η² fashion across a 6:6 ring juncture. Multiple additions have been observed and appear to depend on metal basicity and overall solubility.³

A general feature observed in the solid state structures of fullerenes and their metal complexes has been the inclusion of close-contacting solvent molecules. For example, crystals of C₆₀ grown from benzene contain four benzene solvate molecules per fullerene unit, three of which lie parallel to the C₆₀ surface with C₆₀-C₆H₆ separations less than 3.4 Å.⁴ Also, in the crystal structures of the Vaska-C₆₀ complexes it can be seen that one of the phosphine phenyl rings is tilted toward the fullerene, indicating an attractive π-π interaction. Along these lines, it has also been shown that a supramolecular host/guest complex is possible where the substituted (benzyloxy)benzyl arms of a Vaska derivative wrap around a fullerene in the solid state.⁵ Since the metallofullerene complex precipitates upon addition of C₆₀, it is not clear whether this interaction exists in solution.

Further evidence for arene-fullerene interactions has been observed for the unusual double-addition products⁶ C₆₀{Ir(CO)-

Cl(PPhMe₂)₂}₂·C₆H₆ and C₆₀{Ir(CO)Cl(PPhMe₂)₂}₂·2C₆H₆. In the first complex, there are intimate face-to-face phenyl-C₆₀ interactions without solvent participation, while the second structure shows no phenyl-C₆₀ interaction but has two attractive edge-to-surface benzene-fullerene interactions. Both, the edge-to-surface and face-to-face phenyl-C₆₀ features have been observed in the structure of C₆₀·6SbPh₃.⁷

In all the reported studies regarding C₆₀ additions to Ir(CO)-Cl(PR₃)₂ complexes there has been little or no investigation of solution state binding properties. This is likely due to the poor solubility of the metallofullerene product or the subsequent decomplexation of the iridium center from the fullerene upon dissolution. By using heavily modified phosphine ligands, we were able to investigate the thermodynamic properties of fullerene binding to Vaska type complexes in solution. In this work, we report the synthesis of two (benzyloxy)benzyl dendrimer-containing phosphine derivatives of *trans*-Ir(CO)Cl-(PPh₂R)₂ and their dynamic C₆₀ binding. To our knowledge, this is the first reported example of reversible C₆₀ binding for which thermodynamic values were measured.

Experimental Section

Materials. [G-1]-Br, [G-2]-Br,⁸ and Pd(NCPh)₂Cl₂⁹ were prepared by a literature procedures. ClPPh₂ and Na₃IrCl₆ were purchased from the Strem Chemical Group and used without purification. C₆₀ was purchased from Southern Chemical and used as received. All solvents were dried and degassed using standard procedures.

Measurements. ³¹P{¹H} NMR spectra were recorded on a Varian Unity Plus 500 MHz NMR spectrometer operating at 202.14 MHz and are referenced to an aqueous 85% H₃PO₄ external standard using the positive downfield convention. ¹H NMR spectra were recorded on a General Electric QE-300 NMR spectrometer at 300 MHz. Chemical shifts are relative to tetramethylsilane as an internal reference. Infrared measurements were obtained in CHCl₃ solution or KBr pellets on a Perkin-Elmer Paragon 1000 spectrophotometer. GCMS data were acquired on a Hewlett-Packard 5890 spectrometer.

[®] Abstract published in *Advance ACS Abstracts*, January 15, 1997.

- (1) (a) Fagan, P. J.; Calabrese, J. C.; Malone, B. *Science* **1991**, *252*, 1160. (b) Hawkins, J. M.; Loren, S.; Meyer, A.; Nunlist, R. *J. Am. Chem. Soc.* **1991**, *113*, 7770. (c) Hawkins, J. M.; Meyer, A.; Lewis, T. A.; Loren, S.; Hollander, F. J. *Science* **1991**, *252*, 5003. (d) Fagan, P. J.; Calabrese, J. C.; Malone, B. *J. Am. Chem. Soc.* **1991**, *113*, 9408.
- (2) (a) Balch, A. L.; Catalano, V. J.; Lee, J. W. *Inorg. Chem.* **1991**, *30*, 3980. (b) Balch, A. L.; Catalano, V. J.; Lee, J. W.; Olmstead, M. M.; Parkin, S. R. *J. Am. Chem. Soc.* **1991**, *113*, 8953. (c) Balch, A. L.; Ginwalla, A. S.; Lee, J. W.; Noll, B. C.; Olmstead, M. M. *J. Am. Chem. Soc.* **1994**, *116*, 2227.
- (3) (a) Balch, A. L.; Lee, J. W.; Noll, B. C.; Olmstead, M. M. *Inorg. Chem.* **1994**, *33*, 5238. (b) Balch, A. L.; Hao, L.; Olmstead, M. M. *Angew. Chem., Int. Ed. Engl.* **1996**, *35*, 188. (c) Fagan, P. J.; Calabrese, J. C.; Malone, B. *J. Am. Chem. Soc.* **1991**, *113*, 9408.
- (4) (a) Meidine, M. F.; Hitchcock, P. B.; Kroto, H. W.; Taylor, R.; Walton, D. R. M. *J. Chem. Soc., Chem. Commun.* **1992**, 1534. (b) Balch, A. L.; Lee, J. W.; Noll, B. C.; Olmstead, M. M. *J. Chem. Soc. Chem. Commun.* **1993**, 56.
- (5) Balch, A. L.; Catalano, V. J.; Lee, J. W.; Olmstead, M. M. *J. Am. Chem. Soc.* **1992**, *114*, 5455.

(6) Balch, A. L.; Lee, J. W.; Noll, B. C.; Olmstead, M. M. *J. Am. Chem. Soc.* **1992**, *114*, 10984.

(7) Fedurco, M.; Olmstead, M. M.; Fawcett, W. R. *Inorg. Chem.* **1995**, *34*, 390.

(8) Hawker, C. J.; Fréchet, J. M. J. *J. Am. Chem. Soc.* **1990**, *112*, 7638.

(9) Doyle, J. R.; Slade, P. E.; Jonassen, H. B. *Inorg. Synth.* **1960**, *6*, 216.

General Procedure for the Synthesis of (3,5-Bis(benzyloxy)benzyl)diphenylphosphine or (3,5-Bis((3,5-bis(benzyloxy)benzyl)oxy)benzyl)diphenylphosphine, ((G-*n*)DPP). A 250 mL flask is fitted with an addition funnel, a gas inlet tube, and a mineral oil bubbler. Under nitrogen, 100 mL of anhydrous ammonia is condensed into the flask at $-78\text{ }^{\circ}\text{C}$. Sodium metal (120 mg, 5.21 mmol) is then added, producing a deep blue solution. Chlorodiphenylphosphine (575 mg, 2.60 mmol) is added, and the solution is stirred until bright orange. [G-1]-Br or [G-2]-Br (1 equiv) in dried, degassed tetrahydrofuran (THF) is added dropwise with vigorous stirring. The mixture is removed from the dry ice/acetone bath and allowed to stir at room temperature until the ammonia evaporates. The solvent is then removed under reduced pressure. The residue is redissolved in dichloromethane, the solution filtered through Celite, and the filtrate evaporated to a yellowish oil. The oil is solidified by placing the compound under reduced pressure for a few hours (yield $\sim 70\%$). $\text{PPh}_2(\text{G-1})$: $^{31}\text{P}\{^1\text{H}\}$ NMR (CDCl_3) δ -9.7 ; ^1H NMR (CDCl_3) δ 3.35 (s, 2H, CH_2P), 4.86 (s, 4H, CH_2O), 6.29 (s, 2H, Ar H), 6.35 (s, 1H, Ar H), 7.14–7.41 (m, 22H, Ar H); GCMS, M^+ m/z 488; mp $100\text{--}102\text{ }^{\circ}\text{C}$. $\text{PPh}_2(\text{G-2})$: $^{31}\text{P}\{^1\text{H}\}$ NMR (CDCl_3) δ -9.7 ; ^1H NMR (CDCl_3) δ 3.38 (s, 2H, CH_2P), 4.80 (s, 4H, ArCH_2O), 5.03 (s, 8H, CH_2O), 6.28 (s, 2H, Ar H), 6.38 (s, 1H, Ar H), 6.50 (d, 2H, Ar H, 2 Hz), 6.60 (d, 4H, Ar H, 2 Hz), 7.3–7.44 (m, 30H, Ar H); mp $112\text{--}114\text{ }^{\circ}\text{C}$.

***trans*-IrCl(CO)(PPh₂(G-1))₂, **1**, and *trans*-IrCl(CO)(PPh₂(G-2))₂, **2**.** A 250 mL, three-neck flask fitted with a reflux condenser, a gas inlet tube, and a mineral oil bubbler is charged with $\text{Na}_3\text{IrCl}_6 \cdot 6\text{H}_2\text{O}$ (250 mg, 0.445 mmol) and 100 mL of 2-methoxyethanol. In a well-ventilated fume hood, carbon monoxide (*toxic*) is bubbled through the solution until pale yellow (6–8 h). While the solution is boiled, 2.2 equiv of the appropriate phosphine, $\text{PPh}_2(\text{G-}n)$, is added directly. The mixture is refluxed for 15 min and allowed to cool to room temperature, producing a bright yellow precipitate. Occasionally the product does not separate from the solution. In these instances, the solution is partitioned between dichloromethane and water. The organic layer is removed and dried over anhydrous MgSO_4 , the volume is reduced to 10 mL, and the product is precipitated with EtOH. The product is filtered off and dried under nitrogen. (yield 75%). *trans*-IrCl(CO)(PPh₂(G-1))₂: $^{31}\text{P}\{^1\text{H}\}$ NMR (CDCl_3) δ 22.75; IR $\nu(\text{CO})$ 1961 cm^{-1} . *trans*-IrCl(CO)(PPh₂(G-2))₂: $^{31}\text{P}\{^1\text{H}\}$ NMR (CDCl_3) δ 22.86; IR $\nu(\text{CO})$ 1959 cm^{-1} .

***cis*- and *trans*-PdCl₂(PPh₂(G-1))₂.** To a chloroform solution containing 100 mg (0.261 mmol) of $\text{Pd}(\text{NCPH})_2\text{Cl}_2$ is added dropwise 220 mg (0.574 mmol) of $\text{PPh}_2(\text{G-1})$ dissolved in 20 mL of chloroform. The solution is mildly refluxed for 30 min. The solvent volume is reduced under vacuum, and the product is precipitated with EtOH to give a golden yellow solid (yield 80%). Careful recrystallization from dichloromethane/ethanol precipitates the *trans* isomer: $^{31}\text{P}\{^1\text{H}\}$ NMR (CDCl_3) *cis* δ 20.8, *trans* δ 33.6.

***trans*-PdI₂(PPh₂(G-1))₂.** To a mixture of the above solid dissolved in a minimum amount of dichloromethane is added a methanolic slurry of 10 equiv of NaI. The solution darkens and is stirred for 30 min. The solvent is then evaporated to dryness. The solid is taken up in dichloromethane, the solution filtered through Celite, and the solvent volume reduced under vacuum. Addition of diethyl ether precipitates a single product in nearly quantitative yield: $^{31}\text{P}\{^1\text{H}\}$ NMR (CDCl_3) δ 14.2.

Structure Analyses for *trans*-Ir(CO)Cl(PPh₂(G-1))₂, **1, and PdCl₂(PPh₂(G-1))₂, **3**.** Yellow blocks of **1** and orange blocks of **3** were obtained by slow diffusion of diethyl ether into a chloroform solution of **1** and a dichloromethane solution of **3**, respectively. Crystals were selected and mounted on glass fibers with silicone cement and placed on a Siemens P4 diffractometer. Unit cell parameters were determined by least-squares analysis of 23 reflections with $10.06^\circ < 2\theta < 24.61^\circ$ for **1** and 19 reflections with $7.18^\circ < 2\theta < 21.35^\circ$ for **3**. A total of 4113 reflections were collected for $3.5^\circ < 2\theta < 45^\circ$, yielding 3419 unique reflections ($R_{\text{int}} = 0.0425$) for **1**, while 3027 reflections were collected with $3.5^\circ < 2\theta < 45.0^\circ$, yielding 2467 unique reflections ($R_{\text{int}} = 0.0374$) for **3**. The data were corrected for Lorentz and polarization effects. Crystal data are given in Table 1. Scattering

Table 1. Crystallographic Data for **1** and **3**

	1	3
formula	$\text{C}_{67}\text{H}_{58}\text{ClIrO}_5\text{P}_2$	$\text{C}_{66}\text{H}_{58}\text{Cl}_2\text{O}_4\text{P}_2\text{Pd}$
fw	1232.72	1154.36
<i>a</i> , Å	10.218(1)	10.243(2)
<i>b</i> , Å	12.731(3)	12.689(2)
<i>c</i> , Å	13.116(2)	13.146(2)
α (deg)	112.05(1)	112.33(1)
β (deg)	108.30(1)	108.96(1)
γ (deg)	102.22(1)	101.23(1)
<i>V</i> , Å ³	1392.2(4)	1392.4(4)
space group	$P\bar{1}$	$P\bar{1}$
<i>Z</i>	1	1
<i>D</i> _{calc} , g/cm ³	1.470	1.377
crystal size, mm ³	$0.12 \times 0.26 \times 0.28$	$0.06 \times 0.18 \times 0.24$
$\mu(\text{Mo K}\alpha)$, mm ⁻¹	2.555	0.536
radiation λ , Å	0.710 73	0.710 73
temp, K	298	298
trans factors	0.555–0.775	0.93–0.99
R_1^a, R_2^b ($I > 2\sigma(I)$)	0.0554, 0.0953	0.0480, 0.0716

$$^a R_1 = \sum ||F_o| - |F_c|| / \sum |F_o|. \quad ^b R_2 = [\sum w(F_o^2 - F_c^2)^2 / \sum w(F_o^2)]^{0.5}.$$

factors and corrections for anomalous dispersion were taken from a standard source.¹⁰

Calculations were performed using the Siemens SHELXTL PLUS, version 5.03, system of programs refining on F^2 . The structures were solved by direct methods. In **1**, the carbon monoxide and chloride ligands are disordered across a pseudoinversion center. The chloride was first located in the difference map and assigned an occupancy of 0.5. Subsequent refinement yielded the carbon monoxide which was slightly distorted. The Ir–C and Ir–O bond lengths were fixed at 1.99 and 3.2 Å to yield a better model. This type of disorder is not uncommon in these types of molecules.¹¹ Hydrogen atom positions were calculated using a riding model with a C–H distance fixed at 0.96 Å and a thermal parameter 1.2 times the host carbon atom. An absorption correction was applied using XABS2.¹² All non-hydrogen atoms were refined with anisotropic thermal parameters. For **1**, the largest peak in the final difference map was equivalent to $0.995\text{ e}/\text{\AA}^3$ and was located 1.071 Å from Ir. For **3**, the largest peak in the final difference map was equivalent to $0.364\text{ e}/\text{\AA}^3$ and was located 1.182 Å from P.

Results

Synthesis. As shown in Scheme 1, the dendrimer-containing phosphine ligands are easily constructed using the known dendritic fragments 3,5-bis(benzyloxy)benzyl bromide, [G-1]-Br, and 3,5-bis((3,5-bis(benzyloxy)benzyl)oxy)benzyl bromide, [G-2]-Br, first synthesized by Fréchet.⁸ The phosphines are only mildly air sensitive in solution and are quite soluble in most common organic solvents. $\text{PPh}_2(\text{G-2})$ is significantly more soluble than the smaller $\text{PPh}_2(\text{G-1})$. Both phosphines exhibit similar phosphorus chemical shifts (δ -9.7 ppm), indicating very little difference in electronic nature for the phosphorus atoms in the two compounds. The primary difference between the two species resides in the considerably increased steric bulk in the second-generation compound compared to the first-generation compound. Consequently, $\text{PPh}_2(\text{G-2})$ is considerably more difficult to crystallize and is often obtained as an oil.

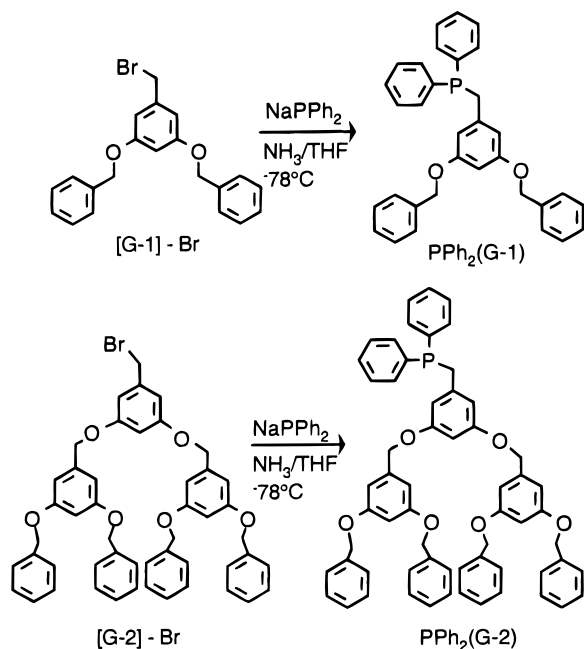
The transition metal complexes are synthesized using standard procedures. The Vaska analogs *trans*-Ir(CO)Cl(PPh₂(G-1))₂, **1**, and *trans*-Ir(CO)Cl(PPh₂(G-2))₂, **2**, are prepared in good yield by carbon monoxide reduction of $\text{Na}_3\text{IrCl}_6 \cdot 6\text{H}_2\text{O}$ in methoxyethanol. The highly soluble, bright yellow complexes are

(10) *International Tables for X-ray Crystallography*; Kynoch Press: Birmingham, England, 1974; Vol. 4.

(11) Churchill, M. R.; Buttry, L. A.; Barkan, M. D.; Thompson, J. S. *J. Organomet. Chem.* **1988**, *340*, 257. Kessler, J. M.; Nelson, J. H.; Frye, J. S.; DeCian, A.; Fischer, J. *Inorg. Chem.* **1993**, *32*, 1048.

(12) XABS2: Parkin, S. R.; Moezzi, B.; Hope, H. *J. Appl. Crystallogr.* **1995**, *28*, 53.

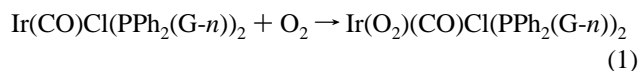
Scheme 1



slightly air sensitive. As expected, both phosphines have similar ³¹P NMR chemical shifts at 22.75 and 22.86 ppm, respectively, as well as carbonyl stretching frequencies in the infrared (~1960 cm⁻¹). It is apparent from these data that the electronic natures of both complexes are very similar as expected.

cis- and *trans*-PdCl₂(PPh₂(G-1))₂ are simply prepared *via* a substitution reaction of Pd(NCPh)₂Cl₂ in chloroform. A mixture of *cis* and *trans* isomers is obtained. The *trans* isomer is precipitated by slow addition of ethanol to a dichloromethane solution of the mixture. Metathesis of the mixture to form the iodo species using methanolic NaI produces the *trans* isomer of PdI₂(PPh₂(G-1))₂ exclusively.

O₂ Studies. As shown in eq 1, complexes **1** and **2** slowly react with O₂ in solution as do Vaska's complex and most of its analogs. The rate of O₂ addition was obtained using



³¹P{¹H} NMR spectroscopy by exposing nitrogen-saturated chloroform solutions of **1** and **2** to air and then taking successive measurements to quantify the formation of Ir(O₂)(CO)Cl(PPh₂(G-*n*))₂. Under pseudo-first-order conditions, plots of ln [Ir-(O₂)] vs time yield straight lines with the slope equivalent to the rate constant. The infrared stretching frequencies at 2010 cm⁻¹ for Ir(O₂)(CO)Cl(PPh₂(G-1))₂ and at 2008 cm⁻¹ for Ir(O₂)(CO)Cl(PPh₂(G-2))₂ are typical values for dioxygen adducts of Vaska analogs. The room-temperature first-order rate constants for O₂ addition were measured 7 × 10⁻⁵ and 3 × 10⁻⁴ s⁻¹ for **1** and **2**, respectively. These values can be compared to 7 × 10⁻⁵ s⁻¹ for *trans*-Ir(CO)Cl(PPh₃)₂ under the same conditions.

C₆₀ Binding. Addition of C₆₀ to bright yellow degassed chlorobenzene solutions of **1** or **2** produces color changes to deep green, typical of C₆₀-Ir(CO)Cl(PPh₂R)₂ complexes. Slow evaporation of the solvent under N₂ produces green/black noncrystalline precipitates. Infrared data for KBr pellets of these precipitates show a single ν(CO) stretch for each compound, 2011 cm⁻¹ for **1** and 2006 cm⁻¹ for **2**, indicating that C₆₀ completely reacted with the iridium complexes in an oxidative-addition fashion. Dissolution of either of these materials in

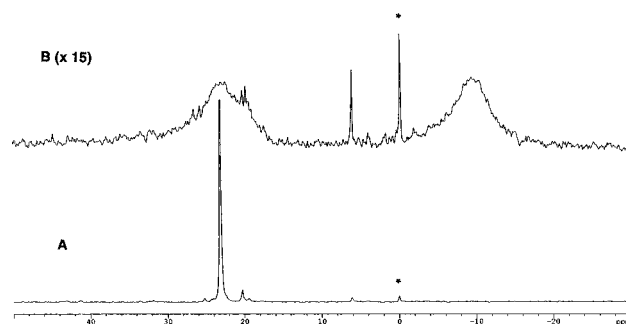


Figure 1. 202.14 MHz ³¹P{¹H} NMR spectra for **1** (spectrum A) recorded in chlorobenzene at 20 °C and after addition of C₆₀ (spectrum B, magnified 15 times). The peak at 5.79 ppm is ligand oxide while the peak labeled * is an unidentified impurity.

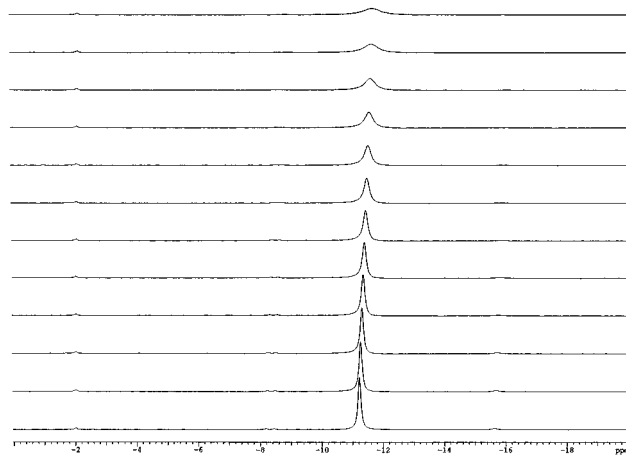
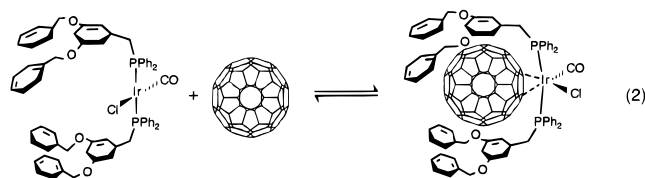


Figure 2. Variable-temperature 202.14 MHz ³¹P{¹H} NMR spectra recorded in chlorobenzene for **2**·C₆₀ in 3° increments from -35 °C (bottom) to -2 °C (top).

chloroform produces a brownish green solution with infrared absorbances identical to those of the starting precursors.

The equilibrium binding of C₆₀ to either **1** or **2** can be examined using variable-temperature ³¹P{¹H} NMR spectroscopy. As shown in Figure 1, addition of C₆₀ to a chlorobenzene solution of **1** at 20 °C (spectrum A) causes the original resonance at 22.86 ppm to broaden significantly, and a new, very broad resonance at ~-12 ppm appears (spectrum A) indicative of the equilibrium shown in eq 2. The small peak at 5.79 ppm has



been identified as the ligand oxide while the other peak labeled with an asterisk is an unidentified impurity. The intensities of both resonances remain constant throughout the experiment. As the solution is cooled further, the equilibrium is shifted to the right, and the original resonance disappears.

The reversible binding was further probed by examining the line width as a function of temperature. Typical data are shown in Figure 2 for **2**·C₆₀ obtained in oxygen-free chlorobenzene between -35 °C (bottom) and -2 °C (top). Other solvent combinations, including toluene or toluene mixtures, caused ligand dissociation from the starting complex. As seen in Figure 2, the resonance for **2**·C₆₀ at -11.8 ppm slowly broadens as the temperature is raised, forcing the equilibrium to the left. The opposite behavior is observed as the temperature is lowered.

Table 2. Thermodynamic Data for C₆₀ Addition to **1** and **2**^a

compd	ΔG_{265}^\ddagger (kcal mol ⁻¹)	ΔH^\ddagger (kcal mol ⁻¹)	ΔS^\ddagger (cal mol ⁻¹ K ⁻¹)
1 ·C ₆₀	1.3	18	20
2 ·C ₆₀	1.3	24	42
compd	ΔG_{265}° (kcal mol ⁻¹)	ΔH° (kcal mol ⁻¹)	ΔS° (cal mol ⁻¹ K ⁻¹)
1 ·C ₆₀	-2.8	-25	-105
2 ·C ₆₀	-3.0	-18	-57

^a Estimated uncertainties are ± 0.2 kcal mol⁻¹ for ΔG , ± 1 kcal mol⁻¹ for ΔH , and ± 5 cal mol⁻¹ K⁻¹ for ΔS .

Table 3. Measured Equilibrium Constants for **1**·C₆₀ and **2**·C₆₀ as a Function of Temperature

1 ·C ₆₀		2 ·C ₆₀	
temp (K)	K (M ⁻¹)	temp (K)	K (M ⁻¹)
263	239	257	388
266	188	261	287
269	99	265	193
272	73	269	104
275	45	273	73
278	27	277	41
281	18	281	22
284	11	285	12
287	4	289	8
290	3	293	5

Similar behavior is seen for **1**·C₆₀ except that the temperature range is different.

Analysis of this array yields the activation data presented in Table 2 according to $k = \pi(\Delta\nu_{\text{cor}})^{13}$ where $\Delta\nu_{\text{cor}}$ is the observed line width minus the natural line width. Plots of line width versus temperature become asymptotic, yielding stopped-exchanged line widths of 14 Hz for **1**·C₆₀ and 64 Hz for **2**·C₆₀. Plots of $\ln(k/T)$ vs $1/T$ are linear. Free energies of reaction of C₆₀ additions to both Ir(CO)Cl(PPh₂(G-1))₂ and Ir(CO)Cl(PPh₂(G-2))₂ are nearly identical at -2.8 and -3.0 kcal mol⁻¹, respectively. A similar study with Vaska's complex is not possible since (C₆₀)Ir(CO)Cl(PPh₃)₂ precipitates out of chlorobenzene.

The equilibrium constant, K_{eq} , was determined as a function of temperature by integration of the ³¹P{¹H} resonances. Selected values are presented in Table 3. At temperatures close to room temperature the equilibrium constants are close to unity. As the temperature is lowered, the equilibrium constants increase by 2 orders of magnitude to 239 mol⁻¹ for **1**·C₆₀ at 263 K and to 388 mol⁻¹ for **2**·C₆₀ at 257 K. Plots of $\ln K_{\text{eq}}$ vs $1/T$ are linear with the slopes yielding ΔH° . The differences between the two complexes is manifested in ΔH° and ΔS° values. The ΔH° value of -25 kcal mol⁻¹ for **1**·C₆₀ is slightly more exothermic than that for **2**·C₆₀, -18 kcal mol⁻¹. The entropies of reaction are both highly negative, with that for **1**·C₆₀ determined to be -105 cal mol⁻¹ K⁻¹ while that for **2**·C₆₀ ΔS° is -57 cal mol⁻¹ K⁻¹. These values can be compared to the activation data presented in Table 2.

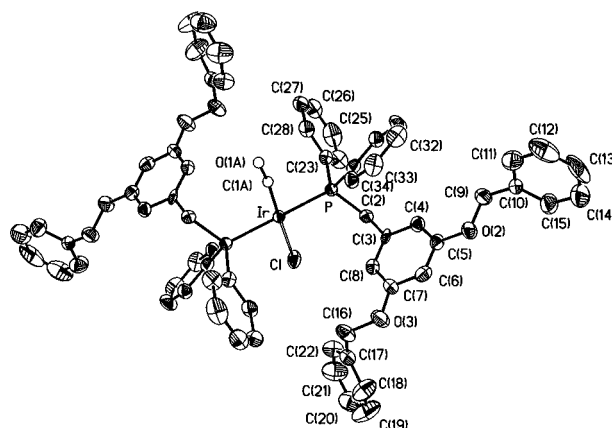
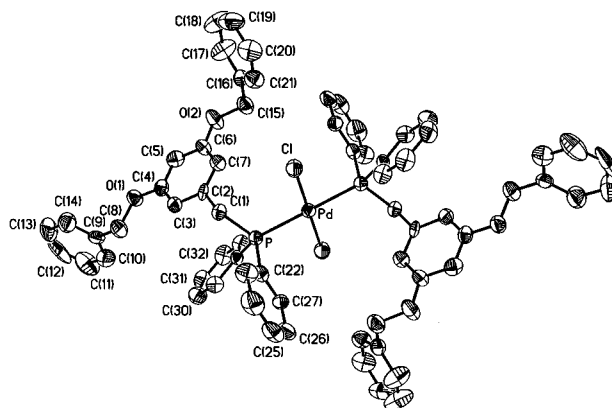
To test whether the addition of C₆₀ to the Vaska analogs was metal dependent or ligand dependent, the ³¹P{¹H} NMR spectrum of a benzene solution of *trans*-PdI₂(PPh₂(G-1))₂ was obtained in both the presence and the absence of C₆₀. Addition of C₆₀ had no effect on the line width or chemical shift of the resonance. In contrast, C₆₀ readily dissolves in a melt of either the G-1 or G-2 phosphine ligand. All attempts to grow crystals from these melts failed.

(13) Kessler, J. M.; Reeder, J. H.; Vac, R.; Yeung, C.; Nelson, J. H.; Frye, J. S.; Alcock, N. W. *Magn. Reson. Chem.* **1991**, *29*, S94.

Table 4. Bond Lengths (Å) and Angles (deg) for **1** and **3**^a

Compound 1			
Ir-C(1)	1.88(3)	Ir-Cl	2.414(11)
Ir-P	2.326(2)	P-C(2)	1.844(9)
P-C(23)	1.817(9)	P-C(29)	1.817(10)
C(1)-Ir-P	91.3(10)	P-Ir-Cl	90.1(2)
C(1)-Ir-Cl	177.7(11)	C(23)-P-Ir	110.0(3)
C(29)-P-Ir	118.9(3)	C(2)-P-Ir	117.7(3)
Compound 3			
Pd-Cl	2.298(2)	P-C(28)	1.812(7)
Pd-P	2.353(2)	P-C(22)	1.824(7)
P-C(1)	1.834(6)		
Cl'-Pd-Cl	180.0	C(28)-P-Pd	119.9(3)
Cl-Pd-P'	89.51(7)	C(22)-P-Pd	108.0(2)
Cl-Pd-P	90.49(7)	C(1)-P-Pd	117.9(2)
P'-Pd-P	180.0		

^a Symmetry transformation used to generate equivalent atoms: (\bar{x} , -y, -z).

**Figure 3.** Thermal ellipsoid plot (40%) of Ir(CO)Cl(PPh₂(G-1))₂, **1**, with hydrogen atoms omitted for clarity. Only one orientation of the disordered CO and Cl groups is shown.**Figure 4.** Perspective view of PdCl₂(PPh₂(G-1))₂, **3**, with 40% thermal contours and hydrogen atoms omitted for clarity.

Structures of *trans*-Ir(CO)Cl(PPh₂(G-1))₂, **1, and *trans*-PdCl₂(PPh₂(G-1))₂, **3**.** Selected interatomic distances and angles are given in Table 4, while atomic coordinates are provided in the Supporting Information. A drawing of *trans*-Ir(CO)Cl(PPh₂(G-1))₂, **1**, is presented in Figure 3, and Figure 4 shows a structural drawing of *trans*-PdCl₂(PPh₂(G-1))₂, **3**. The structures of **1** and **3** are nearly isomorphous, with little distinction between the two. Both molecules are located on a crystallographic center of symmetry with the carbon monoxide and chloride ligands disordered in **1**.

Because of this symmetry, the geometry around the Ir atom in **1** is rigorously square planar and is similar to those of other

Ir(CO)Cl(PR₃)₂ complexes. The phosphines are *trans* to one another with Ir–P separations of 2.326(2) Å. Because of the disorder, an accurate description of the carbonyl geometry is not possible; however, it does not appear to deviate from the expected structure. The distances and angles within the ligand system are also as expected.

Perhaps the most noticeable feature of this structure is the bulk of the phosphine ligands. Even addition of the smallest (benzyloxy)benzyl dendrimer fragment increases the molecular volume substantially. This bulk is directed away from the metal center, and in this regard, the substituted ligand is similar to PPh₃. The estimated cone angle for this phosphine ligand is only ~140°, which can be compared to that of triphenylphosphine (145°).¹⁴

In **3**, the geometry around Pd is also rigorously square planar, with the Cl–Pd–P angle of 90.49°. The Pd–P and Pd–Cl distances are 2.353(2) and 2.298(2) Å, respectively. The intraligand separations are within expected values.

Discussion

The new dendrimer-containing iridium compounds described here show reversible binding to C₆₀, as evidenced by the shift of the carbonyl stretching frequencies, color change to greenish brown, and change in the ³¹P NMR spectra. Attempts to obtain X-ray-quality crystals were thwarted by the high solubility of the complexes in contrast to Vaska's compound, which precipitates under identical conditions. Although the addition of the dendrimer-containing arms to Vaska's compound only mildly alters the electronic properties of the complex, they significantly alter the solubility. It is interesting to note that the metal–fullerene interaction is maintained even in the presence of solvents that nonally cause fullerene precipitation, such as ethers, alkanes, and alcohols.¹⁵ In this regard, the iridium compounds or the redissolved phosphine melts have the potential to act as phase transfer catalysts.

The O₂ addition rate constants for **1** and **2** are not drastically different and are of the same order of magnitude as that for Vaska's compound. In fact, the rate constant for **1** is identical to that for Vaska's complex under similar conditions, indicating that the arms do not protect the metal center much more than triphenylphosphine. This point is reemphasized by noting that the O₂ addition rate for **2** is actually faster than that for **1** even though the phosphine arms are more than twice the steric bulk in **2**. It appears that the larger outer shell of the second-generation dendrimer-containing ligand cannot effectively wrap around the metal center, resulting in a more exposed metal center. Although increasing the number of branches in a dendrimer produces a larger total volume, all of the bulk is

concentrated on the periphery, making the focus quite accessible. This idea has been demonstrated in a polyamidoamine dendrimer which contains voids near the core that are capable of encapsulating guest molecules.¹⁶

The thermodynamic data for C₆₀ addition to the new iridium complexes also indicate that the dendrimer arms do not play a major role in fullerene binding in chlorobenzene solution. There is virtually no difference between the free energies of activation or the free energies of reaction in spite of the large difference in steric bulk of the pendant arms. In fact, Δ*H*[‡] for **2** is only slightly more endothermic than that for **1**, indicating that the iridium–fullerene bonding in the activated complex of **2** is weaker than that in **1**. Further, if the dendrimer arms played any role at all, this would have been manifested in the C₆₀ addition to PdI₂(PPh₂(G-1))₂. Since the PdI₂(PPh₂(G-1))₂ and Ir(CO)Cl(PPh₂(G-1))₂ are isomorphous, the effects of the metal and the ligand can be easily differentiated. The fact that there was no change in the ³¹P line width (8 Hz) upon addition of C₆₀ to PdI₂(PPh₂(G-1))₂ suggests that neither the palladium center nor the benzyloxy arms dictate solution state binding and that the iridium metal is responsible for this interaction. Since no solid state data were obtained, a similar claim for the solid state could not be supported. However, since there is a preponderance of evidence for arene–fullerene (or solvent–fullerene) interactions in the solid state, it is likely that such an interaction would be observed.

The role of the solvent is quite large. It is believed that the large entropy contribution arises from solvent reorganization, and since all experiments were carried out in aromatic solvents, which have an affinity for C₆₀, it is impossible to differentiate solvent competition from dendrimer interaction with the fullerene. Several attempts were made to introduce C₆₀ on both **1** and **2** in nonaromatic solvents, including carbon disulfide, but all cases led to precipitation or degradation. We are currently designing other arene-containing phosphine ligands that would be soluble in hexanes to overcome this problem.

Acknowledgment is made to the donors of the Petroleum Research Fund, administered by the American Chemical Society, for support of this research, to Prof. John H. Nelson and Mr. Lewis W. Cary for assistance, and to Johnson Matthey for a generous loan of iridium salts.

Supporting Information Available: Tables of crystallographic experimental details, atomic coordinates, bond distances, bond angles, anisotropic thermal parameters, hydrogen atom positions, and *U* values for **1** and **3** (11 pages). Ordering information is given on any current masthead page.

IC9612764

(14) Tolman, C. A. *Chem. Rev.* **1977**, *77*, 313.

(15) Ruoff, R. S.; Tse, D. S.; Malhotra, R.; Lorents, D. C. *J. Phys. Chem.* **1993**, *97*, 3379.

(16) Jansen, J. F. G. A.; deDrabner-van den Berg, E. M. M.; Meijer, E. W. *Macromol. Symp.* **1996**, *102*, 27.